From the Radiologic Pathology Archives[1]

Mass Lesions of the Dura: Beyond Meningioma—Radiologic-Pathologic Correlation[2]

Alice Boyd Smith, MD
Iren Horkanyne-Szakaly, MD
Jason W. Schroeder, LCDR, USN, MC
Elisabeth J. Rushing, MD

Abbreviations: AIDS = acquired immunodeficiency syndrome, CNS = central nervous system, EBV = Epstein-Barr virus, ECD = Erdheim-Chester disease, EMA = epithelial membrane antigen, H-E = hematoxylin-eosin, HPC = hemangiopericytoma, PDL = primary dural lymphoma, RDD = Rosai-Dorfman disease, SFT = solitary fibrous tumor, WHO = World Health Organization

RadioGraphics 2014; 34:295–312

Published online 10.1148/rg.342130075

Content Codes: CT MR NR

[1]Supported by the American Institute for Radiologic Pathology (AIRP), the Joint Pathology Center (JPC), and Uniformed Services University of the Health Sciences (USU).

[2]From the Department of Radiology and Radiological Sciences, Uniformed Services University of the Health Sciences, Bethesda, Md (A.B.S.); Department of Neuropathology, Joint Pathology Center, Silver Spring, Md (I.H.S.); Department of Radiology, Walter Reed National Medical Military Center, Bethesda, Md (J.W.S.); and Institute of Neuropathology, University Hospital of Zurich, Zurich, Switzerland (E.J.R.). Received October 5, 2013; revision requested December 23; final revision received January 2, 2014; accepted January 13. For this journal-based SA-CME activity, the authors, editor, and reviewers have no financial relationships to disclose. **Address correspondence to** A.B.S., 2938 Pacific Heights Rd, Honolulu, HI 96813 (e-mail: *absmith@pobox.com*).

Meningioma is the most common mass involving the dura, making it number one in the differential diagnosis for any dural-based mass; however, a variety of other neoplastic and nonneoplastic lesions also involve the dura. Knowledge of the dural anatomy can provide clues to the various processes that may involve this location. The neoplastic processes include both benign and malignant lesions such as hemangiopericytoma, lymphoma, solitary fibrous tumor, melanocytic lesions, Epstein-Barr virus–associated smooth muscle tumors, Rosai-Dorfman disease, and metastatic lesions. The nonneoplastic processes include infectious and inflammatory entities such as tuberculosis and sarcoid, which may mimic mass lesions. In some cases, neoplasms such as gliosarcoma may arise peripherally from the brain parenchyma, appearing dural-based and even inciting a dural tail. Many of these share similar computed tomographic, magnetic resonance imaging, and angiographic characteristics with meningiomas, such as a dural tail, increased vascularity, avid enhancement, and similar signal characteristics; however, knowledge of the patient's age, gender, and underlying conditions and certain imaging characteristics may provide valuable clues to recognizing these lesions. For example, in the population with human immunodeficiency virus infection, Epstein-Barr virus–associated smooth muscle tumors should be included in the differential diagnosis for dural-based lesions. The surgical course and prognosis for these lesions vary, and knowledge of the variety of lesions that involve the dura, their imaging appearances, and their clinical features assists in narrowing the radiologic differential diagnosis and optimizing patient treatment.

SA-CME LEARNING OBJECTIVES FOR TEST 2

After completing this journal-based SA-CME activity, participants will be able to:

- Discuss the differential diagnosis for dural-based lesions.
- Describe the clinical and pathologic features of dural-based lesions.
- List the imaging characteristics of dural-based lesions.

See www.rsna.org/education/search/RG

TEACHING POINTS

See last page

Introduction

The classic dural lesion that is first in everyone's differential diagnosis is the meningioma; however, there are a wide variety of neoplastic and nonneoplastic lesions that involve the dura. The nonneoplastic lesions encompass both noninfectious and infectious etiologies, including tuberculosis and sarcoid. Neoplastic processes include hemangiopericytoma, solitary fibrous tumor, and metastatic lesions. Many dural-based lesions share similar imaging characteristics; however, some have distinctive imaging findings that along with patient history and laboratory findings can guide the radiologist to the appropriate diagnosis.

Dural Anatomy

Knowledge of dural anatomy is key to understanding the histologic features of some of the lesions that involve the dura. The dura mater is a thick, inelastic membrane composed of fibrous and elastic connective tissue that forms the outermost of the three layers of meninges that surround the brain and spinal cord. The dura consists of two layers, the endosteal and meningeal dura, which are fused except where they separate to allow passage of the dural venous sinuses. The endosteal layer adheres closely to bone, contains blood vessels that supply the bone, and functions as an internal periosteum for the calvaria.

The meningeal layer serves as a protective layer for the brain and is lined on its inner surface by a layer of mesothelium similar to that found on serous membranes. Extensions of the cranial dura mater are reduplications of the meningeal layer and project into the cavity of the skull. These processes form the falx cerebri, tentorium cerebelli, falx cerebelli, and diaphragma sellae. A variety of the neoplastic processes involving the dura arise from the various dural components.

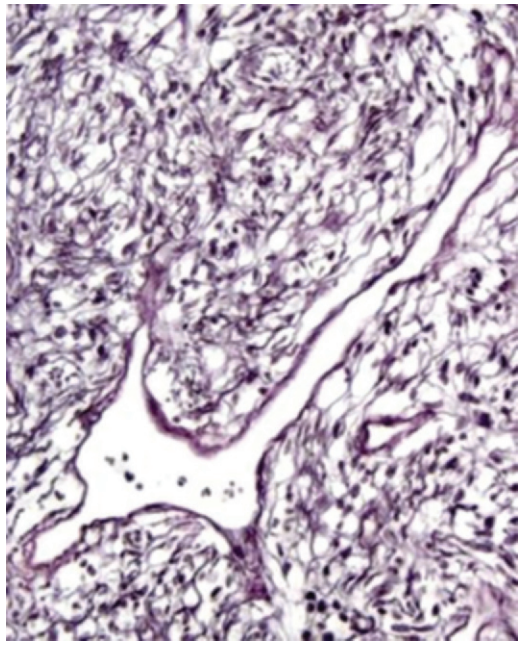

Figure 1. HPC. Photomicrograph (original magnification, ×100; reticulin stain) shows the classic staghorn branching pattern of the vessels and reticulin-rich stroma.

Hemangiopericytoma

Hemangiopericytoma (HPC) is a rare neoplasm that is thought to arise from the Zimmermann pericytes surrounding capillaries and postcapillary venules, but the cell of origin is still controversial (1). These neoplasms more commonly occur in the musculoskeletal system and skin, but rarely occur in the central nervous system (CNS) and account for less than 0.4% of all CNS tumors (2,3). HPCs were originally referred to as *angioblastic meningiomas*, but the name was changed in 1993 to reflect that these lesions are more similar to the soft-tissue hemangiopericytoma than meningiomas (2).

In the general pathology community, HPC is considered part of a spectrum with solitary fibrous tumor (SFT), with HPC representing a more biologically aggressive form. This classification approach has not yet been embraced by neuropathologists and is still under debate. These lesions are classified as World Health Organization (WHO) grade II (HPC) or WHO grade III (anaplastic HPC) lesions. Anaplastic HPC has a higher recurrence rate and the tendency to metastasize outside the CNS, typically to the liver, lungs, and bones, necessitating long-term close clinical and radiologic follow-up (2). More recently, the so-called Marseille criteria propose a new grading system based on extent of resection and pathologic grade (4).

Like meningiomas, HPC is more commonly located supratentorially (5). HPC tends to occur in a younger age group than meningiomas, with average age at presentation of 38–42 years compared with the early 50s for meningioma (6). Approximately 10% of HPCs occur in children and are slightly more common in males (1.4:1) (6,7). Patient presentation depends on the location of the lesion, but symptoms commonly include headache, seizure, visual dysfunction, and motor weakness. Although of limited efficacy, therapy consists of resection and postoperative adjuvant radiation therapy. Owing to their highly vascular nature, preoperative embolization is advisable (8).

Pathologic Features

HPCs are highly cellular, vascular lesions of mesenchymal origin. They are composed of closely packed, randomly oriented cells with scant cytoplasm (2) and interrupted by gaping, capillary-caliber vessels with a branching "staghorn" pattern (Fig 1). The anaplastic form demonstrates greater mitotic activity (≥5 mitoses per 10 high-power fields) or necrosis, along with at least two of the following: hemorrhage, moderate to high nuclear atypia, and cellularity (2,9). According to the Marseille criteria, mitotic activity (>5 per 10 high-power fields) and necrosis alone correlate with outcome. A prominent network of reticulin fibers is a characteristic finding (Fig 1).

Immunohistochemical preparations for CD34 (a transmembrane glycoprotein expressed on hematopoietic progenitor cells, vascular endothelial cells, and some fibroblasts) are focally positive, while stains for epithelial membrane antigen

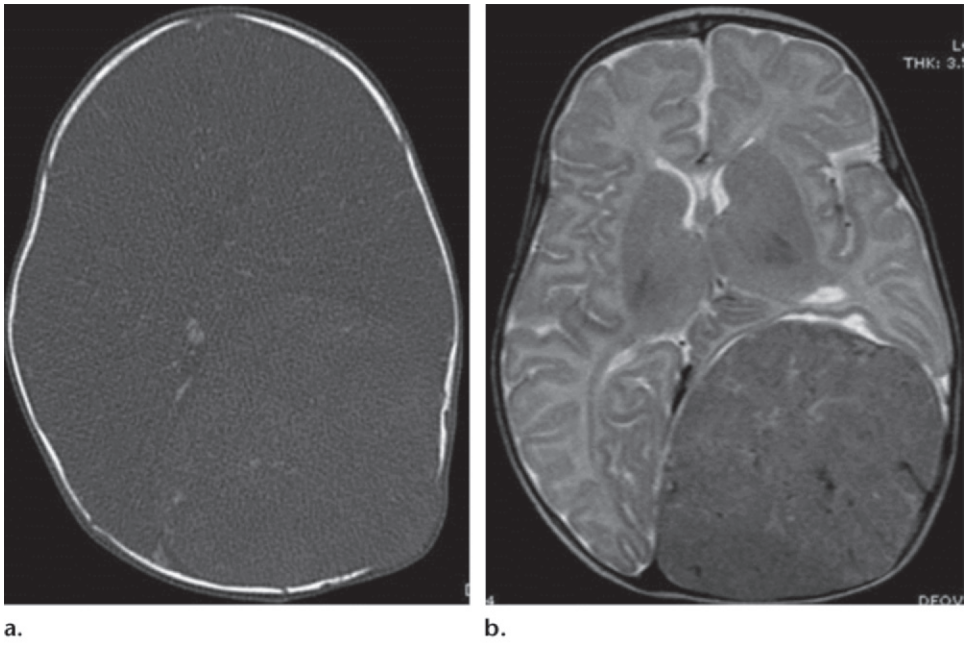

a. b.

c.

Figure 2. HPC in a 2-month-old boy with increasing head circumference. **(a)** Contrast-enhanced computed tomographic (CT) image shows a large extra-axial mass in the left parietal region with osseous erosion and no intratumoral calcifications. **(b)** Axial T2-weighted magnetic resonance (MR) image shows a lesion that is isointense to gray matter. Flow voids are seen within the mass, and there is a mild degree of edema in the adjacent brain parenchyma. **(c)** Postcontrast T1-weighted MR image shows avid enhancement.

(EMA) (a heavily glycosylated, 70-kD protein complex expressed by most glandular and ductal epithelial cells and some hematopoietic cells) are generally negative, which helps distinguish HPC from angiomatous meningioma (10).

Imaging Features

HPCs appear similar to meningioma on imaging, are almost always solitary, and are attached to the dura (2). Rarely, they may be intraparenchymal or intraventricular (2,11). In contradistinction to meningioma, HPC can result in erosion of adjacent bone, as opposed to the hyperostosis that may accompany meningioma, and intratumoral calcification is not seen in HPC (Fig 2a) (12).

Teaching Point

Angiography reveals a hypervascular lesion. HPC is described as having a dual blood supply from both the external carotid artery and either the internal carotid or vertebral artery. These lesions do not typically demonstrate early draining veins, which may be seen in meningiomas, and exhibit what is characterized as a "fluffy" stain versus the "sunburst" stain seen in meningiomas (13). Significant edema is frequently noted in the subjacent brain parenchyma, especially in the atypical form (12,14).

These lesions are typically isointense to gray matter on both T1- and T2-weighted images and prominent flow voids may be seen; due to their vascular nature, they enhance avidly, though sometimes heterogeneously, on postcontrast images (Fig 2b, 2c). When seen, a narrow base of attachment to the dura tends to favor HPC over meningioma, which typically demonstrates a broad base of attachment. "Mushrooming" into the adjacent brain and lobulated or irregular borders also favor HPC (Fig 3a).

In a study by Zhou et al (14) of 39 cases of HPC, lobulated contours, hemorrhage, necrosis, and cystic regions were more common in the anaplastic form. The dural tail sign may be seen and

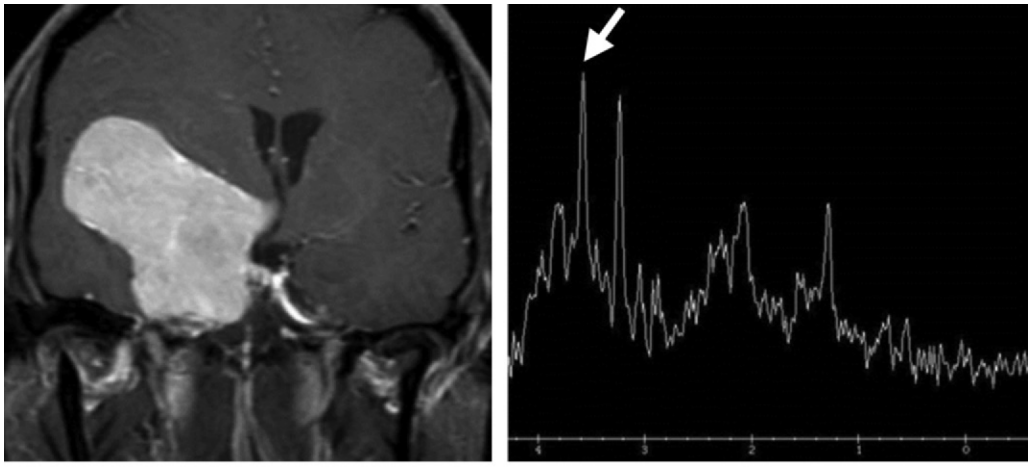

a. b.

Figure 3. HPC in a 32-year-old man with headaches. **(a)** Postcontrast T1-weighted MR image shows an avidly enhancing extra-axial mass with a narrow base compared with the more superior aspect, which is "mushrooming" into the brain. **(b)** Graph from short-echo MR spectroscopy reveals an elevated myo-inositol peak at 3.56 ppm (arrow).

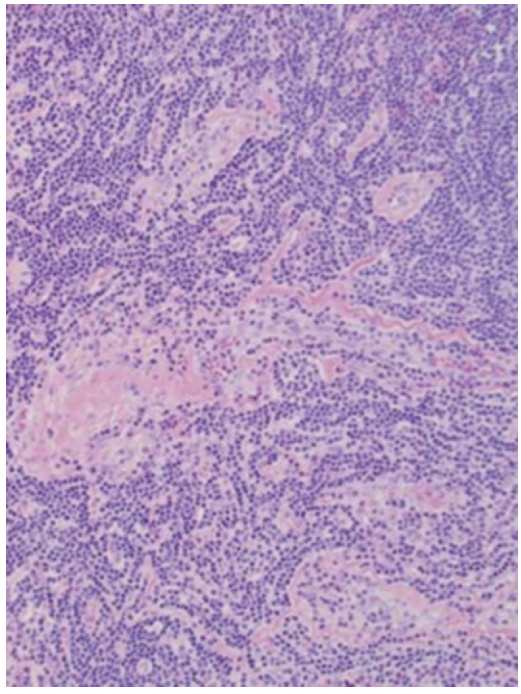

Figure 4. PDL. Photomicrograph (original magnification, ×100; hematoxylin-eosin [H-E] stain) reveals a sheetlike proliferation of neoplastic lymphocytes (small, round, blue-staining cells).

is reported to be more common in grade II lesions (14). The decreased frequency of dural tail in the anaplastic form was postulated to be due to the more rapid growth of these lesions (14). MR spectroscopy demonstrates a high myo-inositol peak at 3.56 ppm and lack of alanine, which may aid in differentiation from meningioma, which has low myo-inositol and demonstrates an alanine peak (8) (Fig 3b).

In a recent study, Liu et al (6) investigated use of the minimum apparent diffusion coefficient (MinADC) to distinguish HPC from meningioma. They found that there was a significant difference in MinADC between HPC ([1.116 ± 0.127] × 10^{-3} mm^2/sec) and meningioma ([0.875 ± 0.014] × 10^{-3} mm^2/sec). They speculated that the higher MinADC in HPC reflects decreased cellularity in comparison with meningioma and abundant vasculature within the tumor matrix.

Lymphoma

Primary dural lymphoma (PDL) is rare, making up less than 1% of all CNS lymphomas (15,16). The majority of PDLs represent the low-grade mucosa-associated lymphoid tissue (MALT) subgroup (17). Since lymphoid tissue is absent in the dura, the pathogenesis of PDL remains unclear. Potential explanations include the following: *(a)* Dural-based MALT lymphoma may result from meningeal seeding from an undiagnosed systemic MALT lymphoma; *(b)* meningothelial cells are embryologically analogous to epithelial cells at other sites in which MALT lymphomas arise, and these cells can be found within the arachnoid membrane and dural venous sinuses; and *(c)* inflammatory conditions involving the dura could attract polyclonal lymphocytes from which MALT lymphoma could arise (17,18).

PDL has a more indolent course than primary CNS lymphoma and is considered a subset of primary leptomeningeal lymphoma, which originates from the meninges without any brain or systemic involvement (16). Most reported

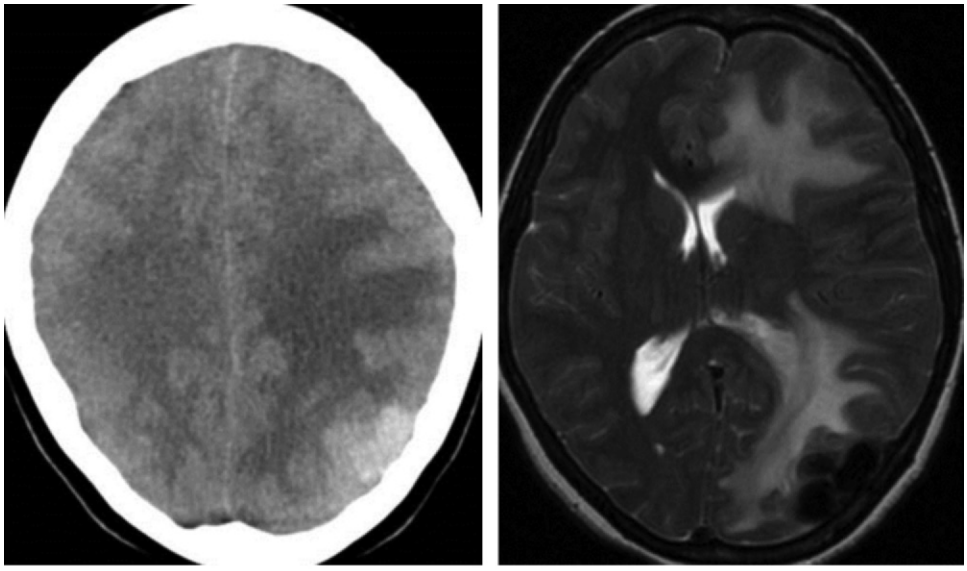

a. b.

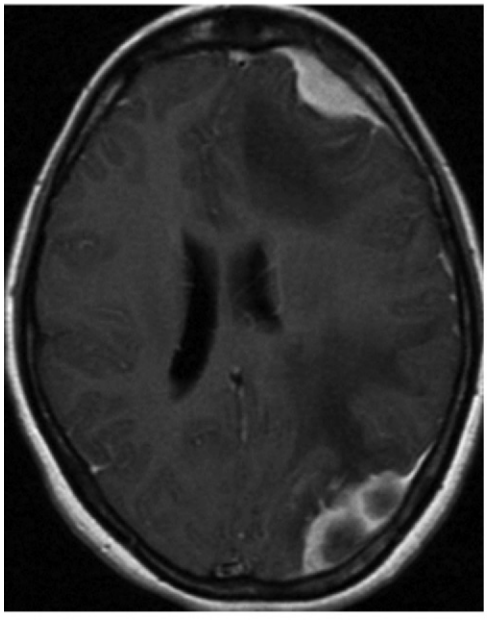

c.

Figure 5. PDL in a 45-year-old woman with headaches. **(a)** Nonenhanced CT image shows a hyperattenuating extra-axial mass in the left parietal region. **(b)** Axial T2-weighted MR image shows a subtle isointense extra-axial mass in the left frontal region with surrounding vasogenic edema. A hypointense, extra-axial mass with surrounding vasogenic edema is seen in the left parietal region, corresponding to the lesion seen at CT. **(c)** Postcontrast T1-weighted MR image shows intense homogeneous enhancement of the frontal lesions and heterogeneous enhancement of the parietal lesions. Dural tails are seen with both.

cases have affected middle-aged females with symptoms and imaging findings mimicking meningiomas (19,20). Patients present with nonspecific neurologic symptoms including headache, meningeal signs, and cranial nerve involvement (21). Regardless of the treatment modality used (surgery or radiation therapy and occasional adjuvant chemotherapy), these neoplasms are reported to have an excellent outcome (17,20). In this way, MALT lymphomas are distinct from other primary CNS or metastatic lymphomas, which typically have a poor outcome.

Pathologic Features

The majority of dural-based lymphomas are low-grade marginal zone lymphomas, but case reports also describe follicular, Hodgkin, and diffuse large B-cell subtypes (16,22,23). In the MALT subtype, histologic evaluation reveals a monomorphous, diffuse infiltrate of small lymphocytes and plasma cells with lymph follicle formation resembling chronic inflammation (Fig 4). They express B-cell–associated antigens such as CD20 and CD79a (17).

Imaging Features

Radiologically, PDL resembles meningioma. Lesions may be single or multiple and are hyperattenuating at CT, reflecting the highly cellular nature of the lesions (Fig 5a). MR imaging reveals iso- to hypointensity on T2-weighted images with avid, although sometimes heterogeneous, enhancement on postcontrast images (Fig 5b, 5c). Vasogenic edema is typically noted in the adjacent brain parenchyma. There may be an indistinct brain-tumor interface, which some suggest may favor PDL over meningioma (24). Occasionally, these tumors may be mistaken for subdural hematomas at nonenhanced CT due to dural location and hyperattenuation (25).

Metastasis

The most common neoplasms to metastasize to the dura are breast, lung, and prostate, but metastases can arise from a variety of other primary neoplasms including melanoma, lymphoma, renal cell, and gastric carcinomas (10,26). Dural metastases are frequently solitary, potentially leading to a misdiagnosis of meningioma and delay in care. (10,27) Pathogenetic mechanisms include hematogenous spread and surgical seeding. Dural involvement from metastases may also result from adjacent metastatic involvement of the skull or brain (10). On rare occasions, tumor-tumor metastases may occur with metastatic deposits found within a meningioma (28). Survival and progression-free survival improve with surgical resection, but survival varies depending on the histology and extent of systemic involvement (27).

Pathologic Features

The histology of metastatic lesions generally reflects that of the primary tumor. For example, an epithelial neoplasm with a ductal growth pattern accompanied by desmoplasia is seen with breast carcinoma, and extensive necrosis with "picket-fence" architecture and goblet cells favors a colorectal primary (10). However, there are potential pitfalls in frozen-section diagnosis in which poorly differentiated metastatic carcinoma may appear similar to anaplastic meningioma and melanoma (10).

Immunohistochemical evaluation that includes transcription factors and hormone receptors can assist in differentiating metastatic carcinomas from anaplastic meningiomas or melanoma (29). Strong, diffuse pancytokeratin (epithelial marker) immunoreactivity with negative EMA supports the diagnosis of metastatic carcinoma (10). Melanoma is considered a great imitator, but can be distinguished from meningioma with various melanoma markers such as HMB-45 and MelanA.

Imaging Features

Dural metastases often manifest as solitary lesions and may have the appearance of linear dural thickening or nodular lesions, with focal or diffuse involvement (10,26). Metastatic dural lesions avidly enhance, reflecting their vascular nature and lack of a blood-brain barrier. A dural tail may be present. Nontraumatic subdural hematoma may rarely be seen (30). The presence of dural enhancement adjacent to osseous involvement may represent dural invasion, but could also be due to a reactive dural response to adjacent metastatic disease. Accordingly, caution should be used when describing dural involvement in these cases (26). Signal intensity depends on the cellularity of the metastatic lesion, with more hypercellular lesions demonstrating lower T2 signal (Fig 6).

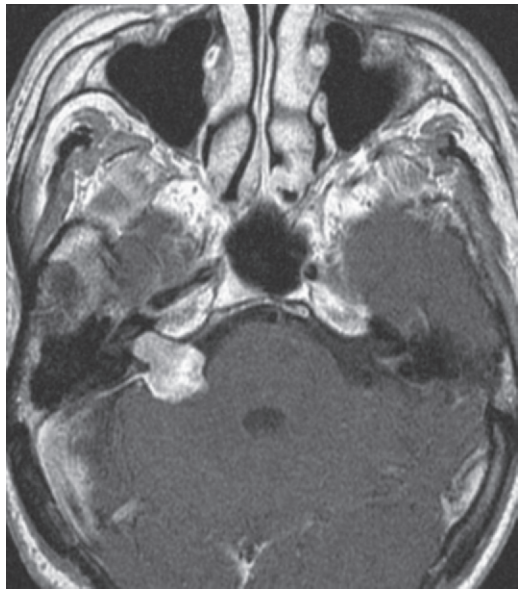

Figure 6. Renal cell metastasis in a 74-year-old man with right-sided hearing loss and a history of resection of a renal neoplasm 10 years earlier. Axial postcontrast T1-weighted MR image shows an avidly enhancing right cerebellopontine mass extending into the right internal auditory canal and demonstrates a dural tail. A second dural-based lesion was seen adjacent to the cerebellar vermis.

Lui et al (31) suggest that perfusion imaging may be of benefit in differentiating dural metastases from meningioma by using first-pass wash-in characteristics. They found that relative wash-in time was lower in metastases than in meningiomas.

Rosai-Dorfman Disease

Rosai-Dorfman disease (RDD) is a rare benign histiocytosis that uncommonly involves the CNS, accounting for only 4% of reported cases (32). The majority of patients present with painless bilateral cervical adenopathy and extranodal involvement that includes the nasal cavity, bone, and orbit. Intracranial lesions occur in approximately 40% of cases (33,34). The etiology is unclear, but a popular theory proposes either a reaction to infectious agents or an autoimmune process (35,36).

Extracranial RDD primarily affects children and young adults with a slight male predominance. Intracranial lesions typically present during the 4th–5th decades with a male predominance (3:1) as opposed to meningiomas, which are more common in middle-aged to older women (35,36). Common intracranial locations include the cerebral convexities and the parasagittal, petroclival, and

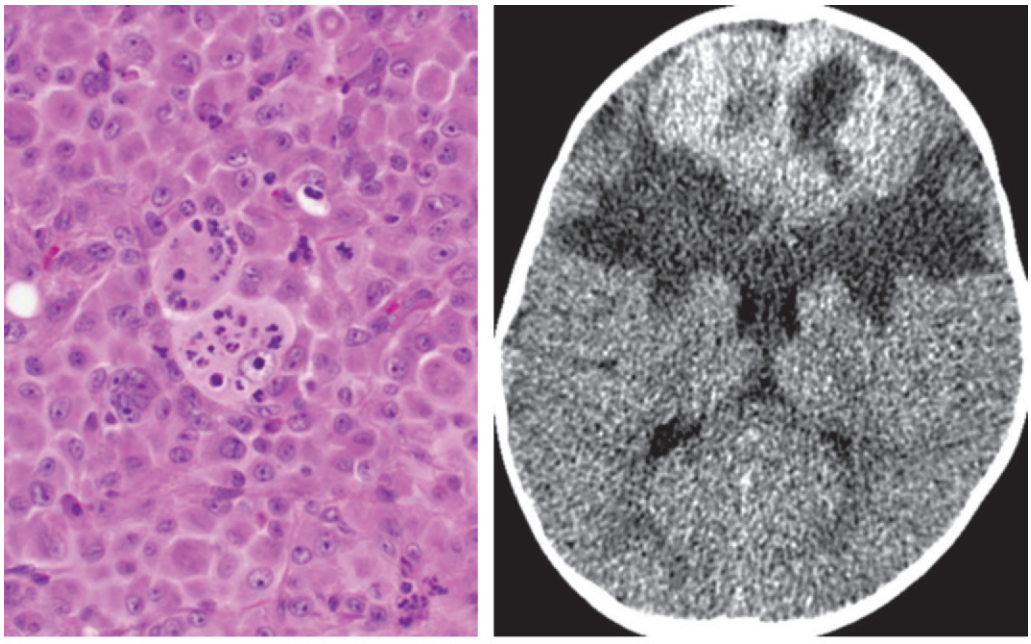

a. b.

Figure 7. RDD in a 28-month-old girl with bilateral papilledema and visual changes. **(a)** Photomicrograph (original magnification, ×40; H-E stain) shows a mixed lymphoplasmacytic infiltrate and a central large pale histiocyte containing intact lymphocytes (emperipolesis). **(b)** Axial nonenhanced CT image shows a hyperattenuating extra-axial mass involving the frontal region with marked vasogenic edema within the adjacent brain.

suprasellar regions (32). Intracranial lesions are more commonly solitary, but multiple lesions are recognized.

Clinical presentation with CNS involvement includes headache, visual change, seizures, numbness, and paraplegia. When the suprasellar region is involved, patients may present with diabetes insipidus (32). Treatment is not well-established but may involve surgery, steroids, chemotherapeutic agents, and radiation. Of these, surgery seems to be the most effective (37).

Pathologic Features

Histologic evaluation frequently reveals a polymorphous infiltrate of lymphoplasmacytic cells and histiocytes of varying size embedded in a fibrous stroma. Of note, emperipolesis (phagocytosis of lymphocytes), which is considered characteristic of RDD, is seen in only 70% of cases (Fig 7a) (38). RDD is characterized by immunoreactivity for S-100 protein (positive in macrophages as well as cells derived from the neural crest, chondrocytes, adipocytes, myoepithelial cells, macrophages, Langerhans cells, dendritic cells, and keratinocytes) and CD68 (marker for cells of macrophage lineage). The lack of immunoreaction for CD1a immunostaining (positive in cortical thymocytes, Langerhans cells, and dendritic reticulum cells) excludes Langerhans histiocyosis, another histologically similar lesion.

Imaging Features

CT reveals a well-circumscribed, dural-based iso- to hyperattenuating mass (Fig 7b). Erosion of adjacent bone has been reported by some, but other series have found no associated erosion, and hyperostosis has not been reported (39,40). These lesions are isointense on T1-weighted images and iso- to hypointense on T2-weighted images, whereas meningiomas tend to be iso- to hyperintense on T2-weighted images. Marked enhancement after contrast material administration is noted, and a dural tail is commonly seen (Fig 8). Lesions may be single or multiple.

Calcification has not been reported as being identified within RDD at either imaging or histologic analysis. Adjacent edema within the brain parenchyma is frequently noted (41). Central low signal intensity on T2-weighted images has been reported, which is postulated to be secondary to release of free radicals by inflammatory macrophages (32). There is limited literature on the angiographic appearance of RDD. However, as compared with the hypervascular appearance of a classic meningioma, RDD tends to demonstrate hypovascularity (42).

Solitary Fibrous Tumor

SFTs are considered benign spindle-cell neoplasms of mesenchymal origin. SFTs have been reported in a variety of locations throughout the

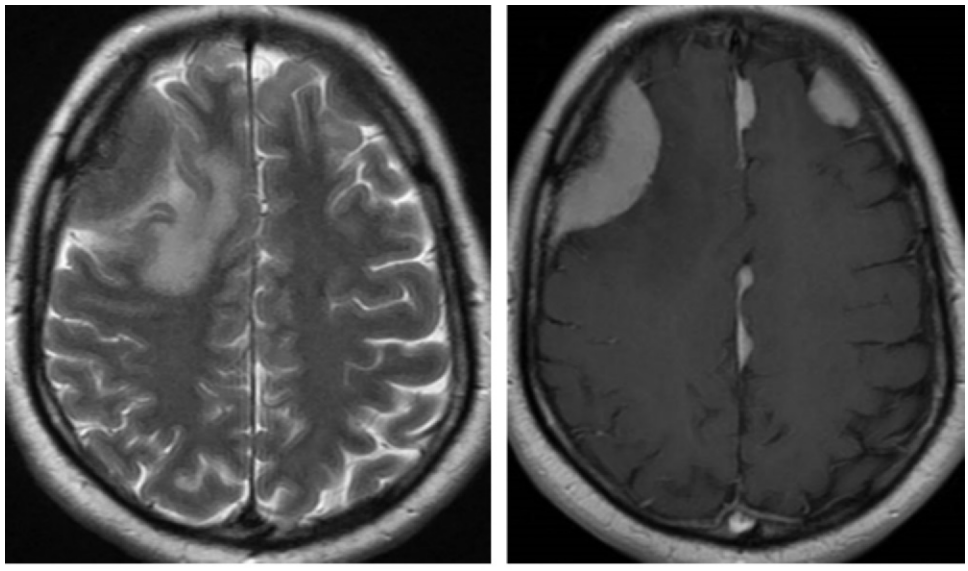

a. b.

Figure 8. RDD in a 37-year-old man with seizure. **(a)** Axial T2-weighted MR image shows a large, hypointense, dural-based mass in the right frontal region with vasogenic edema in the adjacent brain. **(b)** Axial postcontrast T1-weighted MR image shows avid enhancement and small anterior and posterior dural tails. In addition, multiple other dural-based enhancing lesions are noted along the falx and in the left frontal region, which are better appreciated after contrast material administration.

body, including the visceral pleura, liver, skin, orbit, and paranasal sinuses (43). Intracranial location is rare, but when present is often along the dura or within the ventricles. SFTs typically manifest in the same age range as meningiomas (mean age, 57 years), and a strong predilection for women (5:2) has been reported (44–46); however, a recent review of 189 cases by Fargen et al (46) demonstrated no gender predilection.

SFTs are most commonly located along the falx, occipital and spinal dura, tentorium, and at the cerebellopontine angle (45). The most common presentation for an intracranial SFT is headache (43). Surgical removal is the treatment of choice, and postsurgical radiation therapy may be used for residual tumor or unresectable recurrence (47). In the review by Fargen et al (46), approximately 5.8% of CNS SFTs were malignant (46).

Pathologic Features

Although the gross and imaging appearance are those of a well-circumscribed mass, the lesions are not encapsulated (Fig 9a). SFT may appear similar to fibrous meningioma; however, the presence of spindle cells with broad strips of intercellular collagen, diffuse CD34 positivity, and EMA negativity helps distinguish SFT from meningioma (48). Some examples show alternating hypocellular regions with abundant collagen and other areas that are densely hypercellular (Fig 9b). Occasionally, SFTs may demonstrate a more aggressive histologic appearance with necrosis, hemorrhage, and a high mitotic index (46). SFT outside the CNS is considered at the benign end of the spectrum with HPC.

Imaging Features

CT reveals an iso- to hyperattenuating, well-circumscribed lesion that may contain intratumoral calcifications (Fig 9c). Smooth erosion of the adjacent skull may be seen, in contradistinction to the hyperostosis seen with meningiomas.

SFTs demonstrate heterogeneous signal intensity on T2-weighted images. Areas of low T2 signal that enhance avidly on postcontrast images have been reported and may be suggestive of SFT (Fig 10). At histologic evaluation, these areas correspond to areas of fibrosis with abundant collagen (43). A yin-yang appearance on T2-weighted imaging has been described in lesions with hypocellular (hypointense) and hypercelluar (hyperintense) areas (43). Flow voids are commonly seen. Most lesions diffusely or heterogeneously enhance after contrast material administration, and a dural tail may or may not be present (Fig 9d) (43).

Regions of reduced diffusion may be seen, most likely representing the hypercellular areas (43). Lipid and lactate peaks and elevated myo-inositol (3.5 ppm) have been reported at MR spectroscopy, which may help in differentiation from meningioma, in which an elevated alanine peak (1.5 ppm) and glutamate–glutamic acid

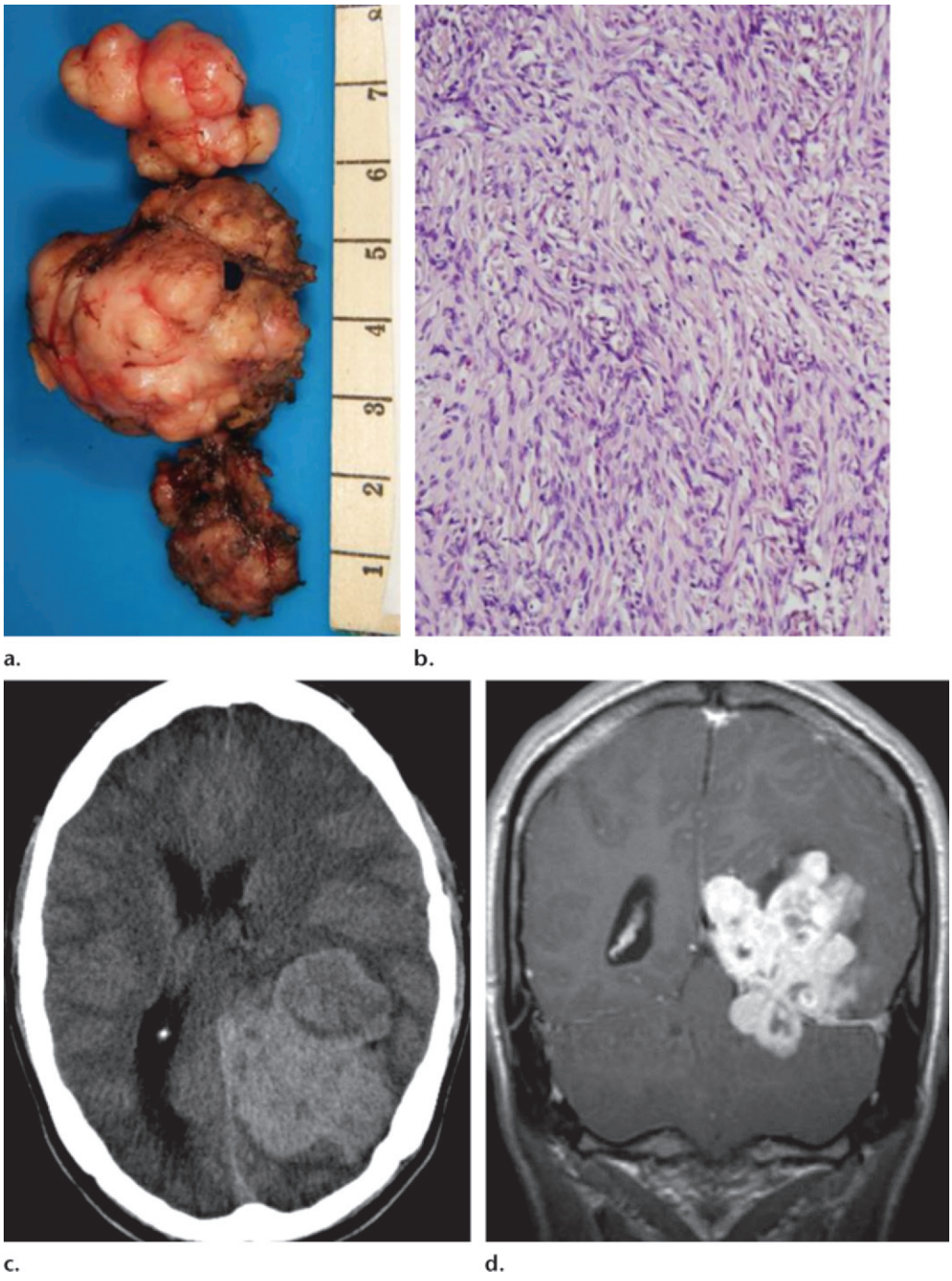

Figure 9. SFT arising from the left aspect of the tentorium in a 28-year-old man with a 4-month history of visual changes and headache. **(a)** Photograph of the gross specimen shows a well-circumscribed lobulated mass. (Scale is in centimeters.) **(b)** Photomicrograph (original magnification, ×40; H-E stain) shows a dense spindle-cell proliferation separated by collagen strips. **(c)** Axial nonenhanced CT image shows a hyperattenuating lobulated mass exerting mass effect on the adjacent brain parenchyma. **(d)** Coronal postcontrast T1-weighted MR image shows avid but heterogeneous enhancement. Association with the tentorium is well-demonstrated and a dural tail is seen.

peak (2.1–2.5 ppm) are seen (43). Elevated myo-inositol is also reported with HPC (49). Perfusion imaging reveals hyperperfusion, and considerable overlap exists between the relative cerebral blood volume (rCBV) of SFTs and meningioma (43).

Depending on location, intracranial SFT may have feeding vessels arising from the pia, external carotid artery, internal carotid artery, or combinations of both internal and external carotid arteries. Prominent tumor blush is usually evident at angiography, leading to preoperative embolization (43,46).

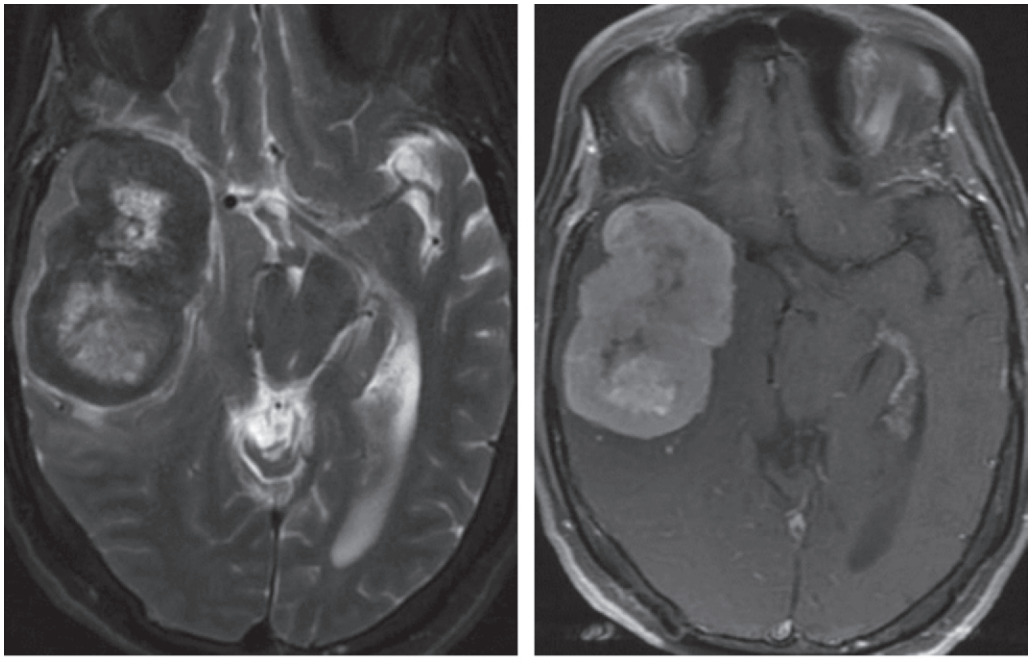

a. b.

Figure 10. SFT in a 68-year-old woman with a 1-year history of temporal headache and dizziness. **(a)** Axial T2-weighted MR image shows a mixed hypo- and hyperintense (yin-yang appearance) extra-axial dural-based mass with mass effect on the adjacent temporal lobe. **(b)** Axial postcontrast T1-weighted MR image shows heterogeneous enhancement, with some of the most avid regions of enhancement corresponding to the T2-hyperintense regions.

EBV-associated Smooth Muscle Tumors

Leiomyoma and leiomyosarcoma are smooth muscle tumors (SMTs) that more commonly involve the uterus, soft tissue, lung, and gastrointestinal tract. These neoplasms rarely involve the CNS, but they are becoming more prevalent in the acquired immunodeficiency syndrome (AIDS) population. They arise from the mesenchymal cells of the dura mater or cerebral blood vessels (50). Coinfection with Epstein-Barr virus (EBV) appears to be necessary for development of these neoplasms, and they are commonly referred to as EBV-associated SMTs (51,52). The mechanism of tumorigenesis has not been elucidated, but is postulated to result from infection and neoplastic transformation of smooth muscle cells by the virus (52).

It has been hypothesized that in the setting of immune compromise, high EBV viral titers at the time of primary infection allowed infection of tissue types that would not normally be infected under normal physiologic conditions (53). These neoplasms have also been identified in post-transplantation and other immune-compromised patients (52,53). It has been reported that EBV-associated SMTs are the second most frequent neoplasm in human immunodeficiency virus (HIV)–positive children (52). Symptoms vary depending on tumor location, and the tumors may be found as an incidental finding at imaging or autopsy. Leiomyoma and leiomyosarcoma should be included in the differential diagnosis of dural-based masses in AIDS patients.

Teaching Point

Pathologic Features

Histologic evaluation of leiomyosarcoma reveals densely packed neoplastic spindle cells with blunt ends and abundant mitotic activity, whereas leiomyoma is composed of fascicles of bland smooth muscle cells. Leiomyosarcoma demonstrates positivity for smooth muscle actin, myogenin (a muscle-specific basic-helix-loop-helix transcription factor), and desmin (a major intermediate filament protein necessary for structural integrity and function of muscle) (10) (Fig 11a, 11b).

Imaging Features

CT shows an isoattenuating dural-based lesion that may contain calcification. At MR imaging, the lesions are hypo- to isointense on T1-weighted images and iso- to hyperintense on T2-weighted imaging. Avid enhancement after administration of contrast material is typically seen, and these lesions share many imaging characteristics with meningiomas (Fig 11c–11e). Case reports have described these lesions as being hypovascular at angiography, unlike meningiomas (54).

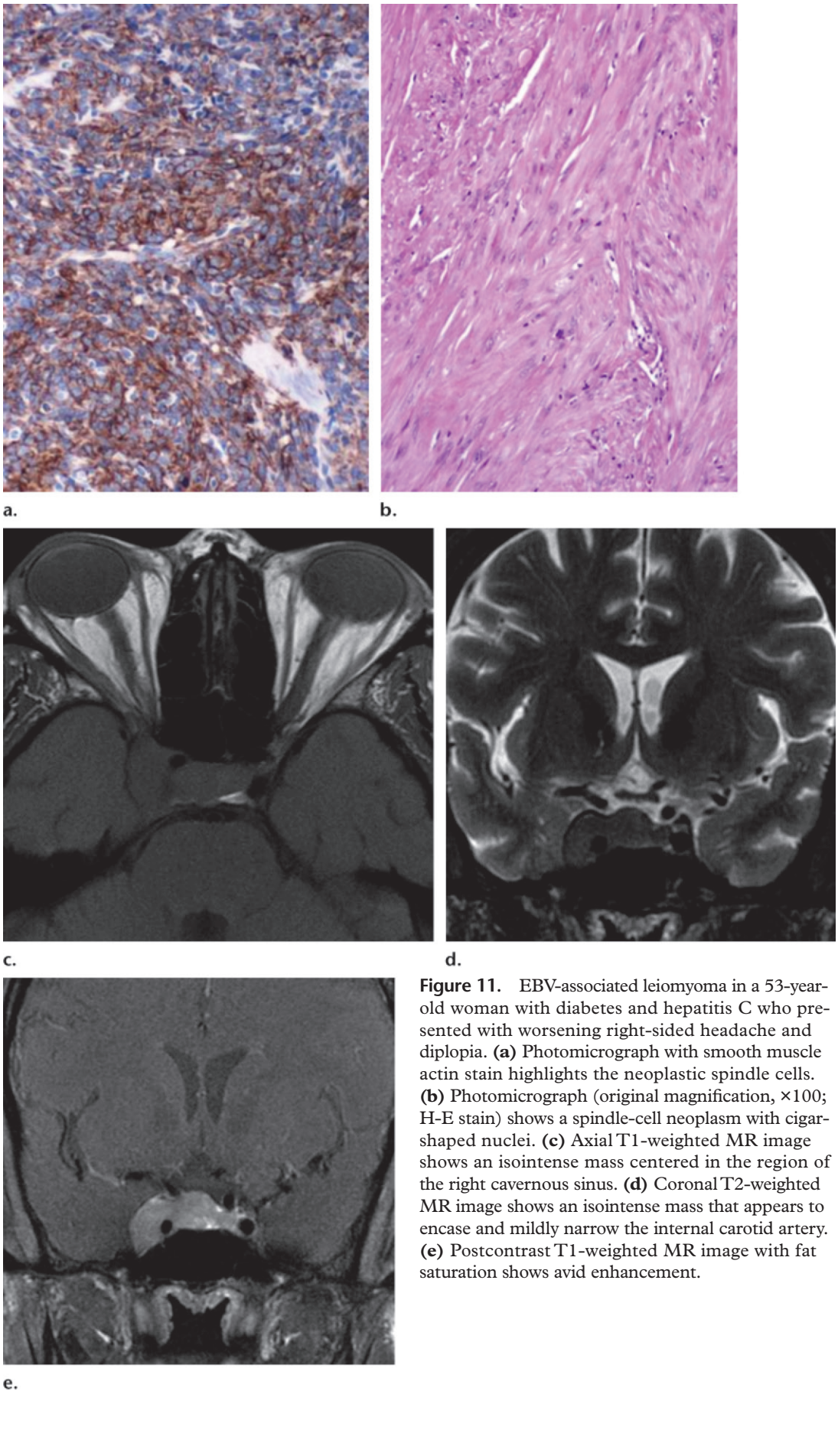

Figure 11. EBV-associated leiomyoma in a 53-year-old woman with diabetes and hepatitis C who presented with worsening right-sided headache and diplopia. **(a)** Photomicrograph with smooth muscle actin stain highlights the neoplastic spindle cells. **(b)** Photomicrograph (original magnification, ×100; H-E stain) shows a spindle-cell neoplasm with cigar-shaped nuclei. **(c)** Axial T1-weighted MR image shows an isointense mass centered in the region of the right cavernous sinus. **(d)** Coronal T2-weighted MR image shows an isointense mass that appears to encase and mildly narrow the internal carotid artery. **(e)** Postcontrast T1-weighted MR image with fat saturation shows avid enhancement.

Melanocytic Neoplasms

Melanocytic lesions of the CNS are rare, and lesions involving the dura include both primary melanocytic lesions and metastatic melanoma. Primary lesions include melanocytoma and primary malignant melanoma. Rarely, melanotic neuroectodermal tumor of infancy may arise from the dura. The histologic characteristics of some lesions may overlap, and it is important to differentiate between primary and metastatic lesions, since the workup and treatment differ. The absence of a known primary helps in this endeavor; however, an occult primary should be sought and excluded.

Melanocytoma is a typically benign lesion arising from resident melanocytic cells found within the leptomeninges. In some cases, malignant behavior has been reported (55). These tumors may occur at any age, but the majority of patients present within the 5th decade of life, and women are affected more often than men (56). The most common sites are the posterior fossa, Meckel cave, and cervical and thoracic spinal canal, probably reflecting the higher concentration of melanocytes in these areas (55). Symptoms depend on location, but often include myelopathy, radiculopathy, seizures, hydrocephalus, and cranial nerve deficits. Treatment is surgical resection, which may be curative, but up to 22% of cases recur within 3 years. If complete resection is not possible or there is a recurrence, radiation therapy is used (57).

Pathologic Features

At gross inspection, melanocytomas are typically darkly pigmented masses (Fig 12a). Histology reveals tight cellular nests or whorls, and abundant melanin pigment may be seen within the cytoplasm (Fig 12b). Differentiating melanocytoma from melanoma may be difficult, but the lack of mitotic activity, nuclear pleomorphism, and hyperchromaticity in combination with an indolent growth pattern favor melanocytoma (58). Immunohistochemical evaluation reveals positivity for melanocytic proteins including S-100, melan-A, and HMB-45, similar to melanoma.

Imaging Features

Melanocytomas are iso- to hyperattenuating at CT, with an imaging appearance similar to meningiomas; however, hyperostosis and intratumoral calcification are rarely seen in melanocytomas (Fig 12c) (55). Avid enhancement occurs after administration of contrast material. At MR imaging, T1 hyperintensity may be seen, reflecting the melanin. The lesions are typically iso- to hypointense on T2-weighted images (Fig 12d–12f).

Erdheim-Chester Disease

Erdheim-Chester disease (ECD) is a rare non–Langerhans cell histiocytosis that more commonly involves the skin and long bones, but other sites of involvement include the cardiopulmonary system, intraperitoneal organs, orbital fossa, and CNS (59). Neurologic involvement is seen in less than 30% of cases and can be divided into three patterns: infiltrative, meningeal, and composite (combined infiltrative and meningeal patterns) (60). The infiltrative type consists of widespread nodules or masses predominantly involving the cerebellum and brainstem. The meningeal form is described as meningioma-like with nodular thickening along the dura. Xanthoma is a localized form of the disease that is composed of foamy (or xanthoma) cells. Dural xanthomas are also seen in the setting of familial hypercholesterolemia and Weber-Christian disease.

ECD typically affects patients in the 5th decade of life (age range, 7–84 years; mean, 53 years), and men are more commonly affected than women (3:1) (61). The clinical course varies with the extent of the disease. Some patients never develop clinical symptoms and the disease is discovered incidentally. However, when patients have neurologic involvement they are often symptomatic, with diabetes insipidus (seen with pituitary involvement) and ataxia being the most common manifestations (62,63). The treatment is controversial, but surgical resection and radiation therapy have been used (64).

Pathologic Features

Histologic analysis reveals collections of large histiocytes with clear, foamy cytoplasm (xanthoma cells) in a background of fibrosis (Fig 13a). The immunohistologic characteristics of ECD differ from Langerhans cell histiocytosis. The histiocytes of ECD are CD68 positive, CD1a (T-cell surface antigen used to diagnosis Langerhans cell histiocytosis) negative, and do not immunostain for S-100 protein (63).

Imaging Features

Single or multiple dural-based masses may be seen, and diffuse pachymeningeal thickening may be associated. The lesions are iso- to slightly hypointense on T1-weighted images and avidly and homogeneously enhance after administration of gadolinium contrast material. It has been reported that the enhancement may persist for up to 8 days after injection of contrast material. This finding is postulated to be secondary to retention of gadolinium by the histiocytes (63,65). On T2-weighted imaging, ECD is iso- to hypointense (63) (Fig 13b, 13c).

Owing to the systemic nature of ECD, multiple sites are frequently involved. In a series by Drier et al (63), all of the patients with intracranial

Teaching Point

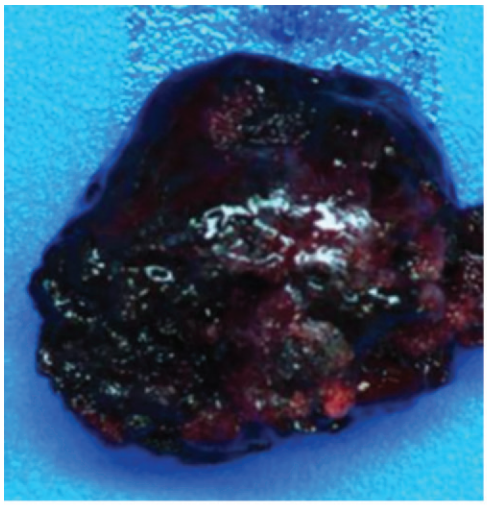

a.

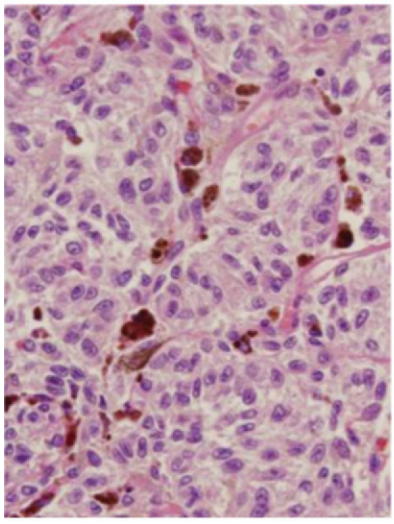

b.

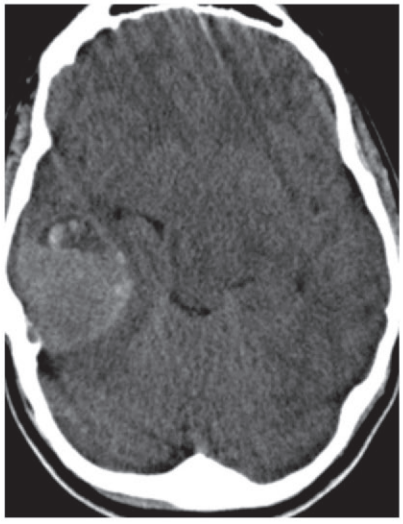

c.

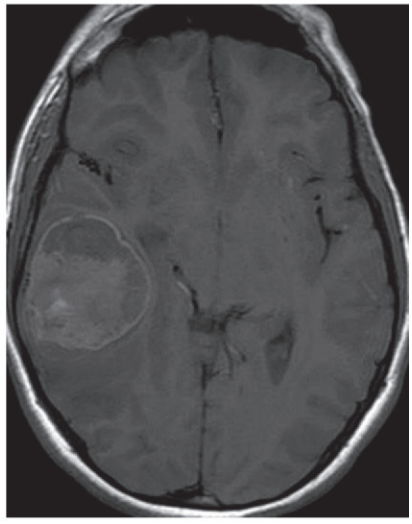

d.

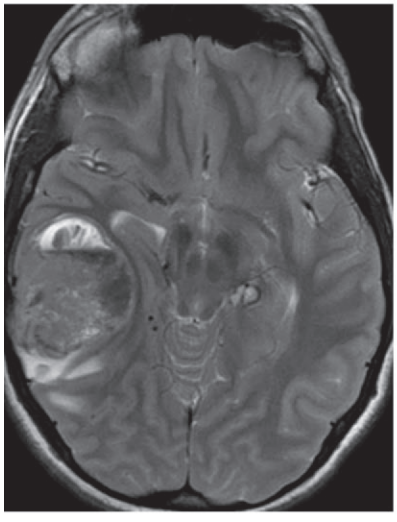

e.

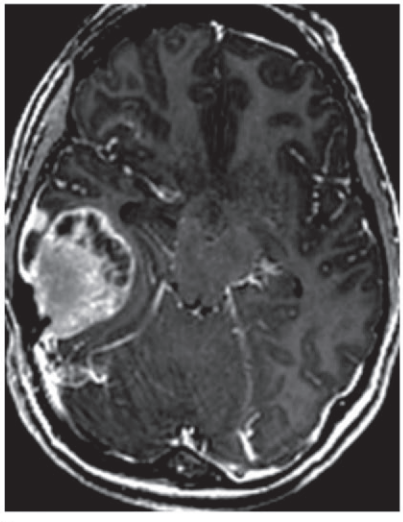

f.

Figure 12. Melanocytoma in a 34-year-old man with seizure. **(a)** Photograph of the gross specimen shows a deeply pigmented well-circumscribed tumor. **(b)** Photomicrograph (original magnification, ×100; H-E stain) shows nests of bland-appearing cells with melanin granules in the cytoplasm. **(c)** Axial nonenhanced CT image shows a predominantly hyperattenuating extra-axial mass causing mass effect on the right temporal lobe and midbrain. **(d)** Axial T1-weighted MR image shows that the lesion is predominantly hyperintense. **(e)** Axial T2-weighted MR image shows a predominantly isointense mass. A mild degree of edema is noted in the adjacent brain. **(f)** Postcontrast T1-weighted MR image shows avid enhancement of the majority of the lesion. A dural tail is seen both anterior and posterior to the mass.

lesions had osteosclerosis of the sinus walls or orbital masses. Therefore, if lesions are also noted to involve the facial bones or orbits, it is suggestive of ECD.

Sarcoid

Sarcoidosis is a systemic disease of unknown origin characterized by the formation of noncaseating granulomas. It is theorized that it may represent

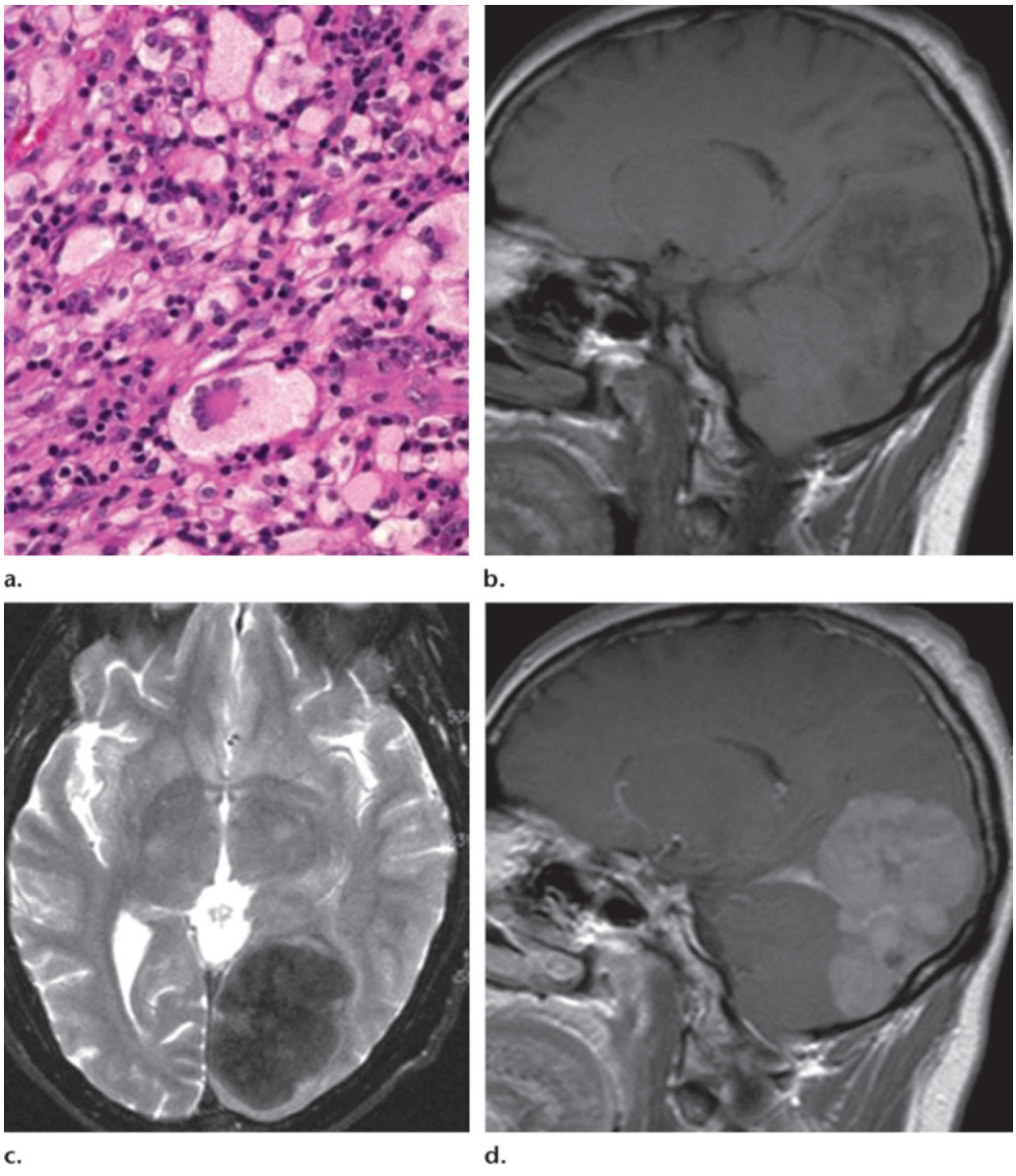

Figure 13. ECD in a 49-year-old man with intermittent headaches and dizziness. **(a)** Photomicrograph (original magnification, ×100; H-E stain) shows collections of foamy histiocytes accompanied by a variable lymphocytic infiltrate. **(b)** Sagittal T1-weighted MR image shows a slightly hypointense extra-axial mass extending superiorly and inferiorly from the tentorium and exerting a localized mass effect on the occipital lobe and cerebellum. **(c)** Axial T2-weighted MR image shows a markedly hypointense mass. **(d)** Postcontrast MR image shows homogeneous enhancement of the lesion. A dural tail is seen anteriorly.

an immune-mediated response to an as of yet unidentified antigen (66). There is a bimodal age distribution, with the initial peak around 20–29 years and the second peak in women older than 50 years (67). Sarcoidosis is slightly more common in females and nearly threefold more common in blacks than in whites (67,68).

Asymptomatic CNS involvement is noted in up to 25% of autopsies, and clinical involvement occurs in about 5% of cases. Isolated neurosarcoidosis without signs of systemic disease is extremely rare, occurring in less than 1% of cases (69,70). Neurosarcoidosis has a predilection for the basilar meninges, but any portion of the CNS can be involved (69). Dural involvement may be diffuse or focal and mass-like, and the mass-like involvement of the dura may mimic a meningioma or nerve sheath tumor.

Manifestations of neurosarcoid depend on site and extent, but headaches and cranial nerve involvement are some of the more common symptoms. Owing to its nonspecific clinical presentation and neuroradiologic imaging characteristics, neurosarcoid is a difficult diagnosis to confirm,

Teaching Point

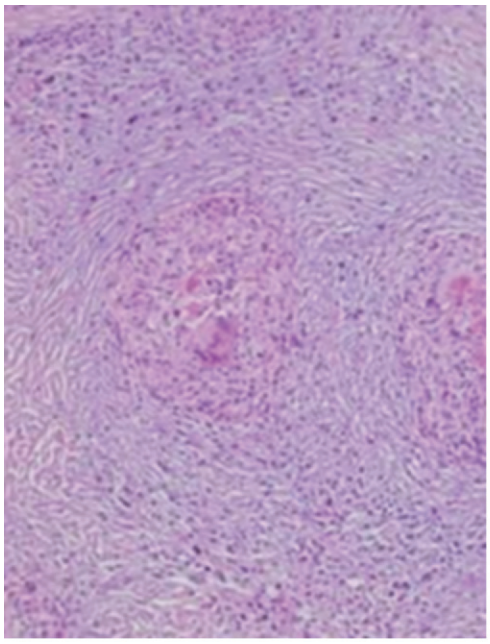

a.

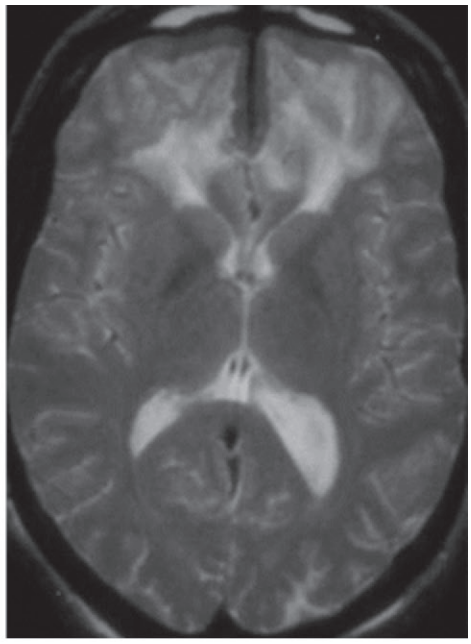

b.

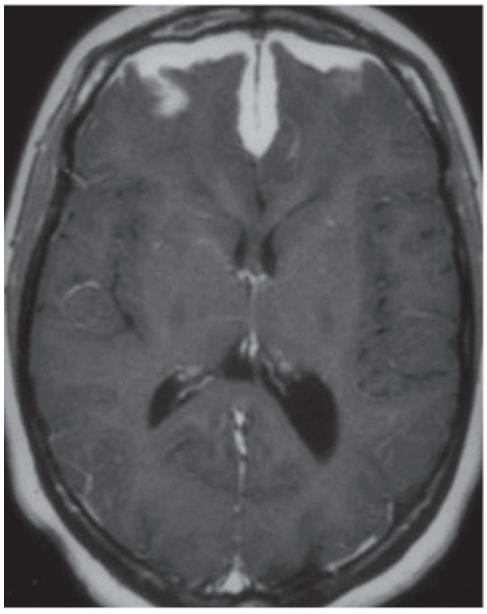

c.

Figure 14. Neurosarcoidosis in a 53-year-old woman with headaches. **(a)** Photomicrograph (original magnification, ×40; H-E stain) shows a noncaseating granuloma with a central core of epithelioid histiocytes and a giant multinucleated cell surrounded by lymphocytes (small blue cells). **(b)** Axial T2-weighted MR image shows a plaque-like hypointense lesion involving the frontal dura. **(c)** Postcontrast image shows avid enhancement. Leptomeningeal involvement with extension into the sulci is seen on the right.

especially in the absence of systemic disease (69). Lumbar puncture may be useful in ruling out other neurologic disorders, but the findings in neurosarcoid are nonspecific (high protein, high leukocyte count, and normal or low glucose) and in up to 30% of cases may be normal (69). Performing chest imaging to evaluate for pulmonary involvement may be helpful. No controlled trials of treatment of neurosarcoid have been performed; however, corticosteroids are considered the first line of treatment (71).

Pathologic Features

Gross examination reveals dural or leptomeningeal thickening. The cardinal histologic finding in neurosarcoid is the presence of noncaseating granulomas infiltrating the meninges (Fig 14a). Unfortunately, this is not a specific finding, and exclusion of caseating necrosis (a feature of tuberculosis), foreign bodies, and organisms is necessary. Special stains and cultures of acid-fast bacilli and fungi should be performed.

Imaging Features

Imaging of dural lesions typically reveals diffuse thickening or a focal mass, which tend to be isointense to gray matter on T1-weighted images and hypointense on T2-weighted images. Postcontrast imaging reveals homogeneously enhancing lesions (Fig 14b, 14c). The low signal intensity on T2-weighted images is thought to be secondary to accumulation of fibrocollagenous material (66).

Other Dural Lesions

A variety of other lesions can involve the dura. These include neoplastic entities such as leukemia or peripherally based intra-axial neoplasms such as gliosarcoma (Fig 15). Amyloid and rheumatoid nodules are rarely found involving the

dura. Uncommonly, infectious processes involving the dura may result in a mass-like lesion that mimics a meningioma. Tuberculosis and syphilis are two examples that can result in a mass-like lesion, especially in the setting of immune compromise.

Conclusion

A wide variety of lesions can involve the dura, ranging from benign to malignant neoplastic, infectious, and granulomatous etiologies. Frequently, these lesions have imaging characteristics similar to those of a meningioma and are often mistaken for one. Many of these lesions demonstrate lower T2 signal intensity than meningiomas and do not result in hyperostosis, which should offer a clue. A high degree of suspicion along with the clinical history may help in distinguishing these lesions.

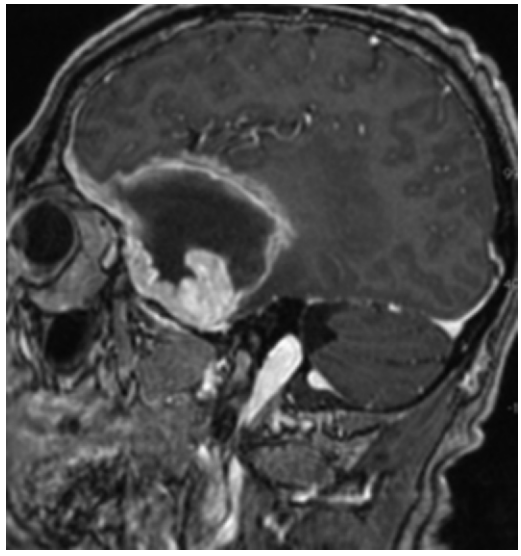

Figure 15. Gliosarcoma in a 60-year-old man with a seizure. Sagittal postcontrast T1-weighted MR image shows a peripherally located mass in the anterior right temporal lobe with predominantly peripheral enhancement due to central necrosis. A dural tail is present.

References

1. Stout AP, Murray MR. Hemangiopericytoma: a vascular tumor featuring Zimmerman's pericytes. Ann Surg 1942;116(1):26–33.
2. Giannini C, Rushing EJ, Hainfellner JA. Haemangiopericytoma. In: Louis DN, Ohagaki H, Wiestler OD, Cavanees WK, eds. WHO classification of tumours of the central nervous system. Lyon, France: IARC, 2007; 178–180.
3. Goellner JR, Laws ER Jr, Soule EH, Okazaki H. Hemangiopericytoma of the meninges: Mayo Clinic experience. Am J Clin Pathol 1978;70(3):375–380.
4. Bouvier C, Métellus P, de Paula AM, et al. Solitary fibrous tumors and hemangiopericytomas of the meninges: overlapping pathological features and common prognostic factors suggest the same spectrum of tumors. Brain Pathol 2012;22(4):511–521.
5. Perry A, Scheithauer BW, Nascimento AG. The immunophenotypic spectrum of meningeal hemangiopericytoma: a comparison with fibrous meningioma and solitary fibrous tumor of meninges. Am J Surg Pathol 1997;21(11):1354–1360.
6. Liu G, Chen ZY, Ma L, Lou X, Li SJ, Wang YL. Intracranial hemangiopericytoma: MR imaging findings and diagnostic usefulness of minimum ADC values. J Magn Reson Imaging 2013;38(5):1146–1151.
7. Guthrie BL, Ebersold MJ, Scheithauer BW, Shaw EG. Meningeal hemangiopericytoma: histopathological features, treatment, and long-term follow-up of 44 cases. Neurosurgery 1989;25(4):514–522.
8. Barba I, Moreno A, Martinez-Pérez I, et al. Magnetic resonance spectroscopy of brain hemangiopericytomas: high myoinositol concentrations and discrimination from meningiomas. J Neurosurg 2001;94(1):55–60.
9. Mena H, Ribas JL, Pezeshkpour GH, Cowan DN, Parisi JE. Hemangiopericytoma of the central nervous system: a review of 94 cases. Hum Pathol 1991;22(1):84–91.
10. Savage NM, Alleyne CH, Vender JR, et al. Dural-based metastatic carcinomas mimicking primary CNS neoplasia: report of 7 cases emphasizing the role of timely surgery and accurate pathologic evaluation. Int J Clin Exp Pathol 2011;4(5):530–540.
11. Abrahams JM, Forman MS, Lavi E, Goldberg H, Flamm ES. Hemangiopericytoma of the third ventricle: case report. J Neurosurg 1999;90(2):359–362.
12. Fountas KN, Kapsalaki E, Kassam M, et al. Management of intracranial meningeal hemangiopericytomas: outcome and experience. Neurosurg Rev 2006;29(2):145–153.
13. Sibtain NA, Butt S, Connor SEJ. Imaging features of central nervous system haemangiopericytomas. Eur Radiol 2007;17(7):1685–1693.
14. Zhou JL, Liu JL, Zhang J, Zhang M. Thirty-nine cases of intracranial hemangiopericytoma and anaplastic hemangiopericytoma: a retrospective review of MRI features and pathological findings. Eur J Radiol 2012;81(11):3504–3510.
15. Zimmerman HM. Malignant lymphomas of the nervous system. Acta Neuropathol Suppl 1975;6(suppl 6):69–74.
16. Said R, Rizk S, Dai Q. Clinical challenges of primary diffuse large B-cell lymphoma of the dura: case report and literature review. ISRN Hematol 2011;2011:945212.
17. Ferguson SD, Musleh W, Gurbuxani S, Shafizadeh SF, Lesniak MS. Intracranial mucosa-associated lymphoid tissue (MALT) lymphoma. J Clin Neurosci 2010;17(5):666–669.
18. Kumar S, Kumar D, Kaldjian EP, Bauserman S, Raffeld M, Jaffe ES. Primary low-grade B-cell lymphoma of the dura: a mucosa associated lymphoid tissue–type lymphoma. Am J Surg Pathol 1997;21(1):81–87.
19. Altundag MK, Ozişik Y, Yalcin S, Akyol F, Uner A. Primary low grade B-cell lymphoma of the dura in an immunocompetent patient. J Exp Clin Cancer Res 2000;19(2):249–251.
20. Venkataraman G, Rizzo KA, Chavez JJ, et al. Marginal zone lymphomas involving meningeal dura: possible link to IgG4-related diseases. Mod Pathol 2011;24(3):355–366.

21. Lachance DH, O'Neill BP, Macdonald DR, et al. Primary leptomeningeal lymphoma: report of 9 cases, diagnosis with immunocytochemical analysis, and review of the literature. Neurology 1991;41(1): 95–100.
22. Narberhaus B, Buxó J, Pérez de Olaguer J, et al. Primary dural lymphoma [in Spanish]. Neurologia 1996;11(3):117–119.
23. Miranda RN, Glantz LK, Myint MA, et al. Stage IE non-Hodgkin's lymphoma involving the dura: a clinicopathologic study of five cases. Arch Pathol Lab Med 1996;120(3):254–260.
24. Iwamoto FM, DeAngelis LM, Abrey LE. Primary dural lymphomas: a clinicopathologic study of treatment and outcome in eight patients. Neurology 2006;66(11):1763–1765.
25. Gocmen S, Gamsizkan M, Onguru O, Sefali M, Erdogan E. Primary dural lymphoma mimicking a subdural hematoma. J Clin Neurosci 2010;17(3): 380–382.
26. Nayak L, Abrey LE, Iwamoto FM. Intracranial dural metastases. Cancer 2009;115(9):1947–1953.
27. Kleinschmidt-DeMasters BK. Dural metastases: a retrospective surgical and autopsy series. Arch Pathol Lab Med 2001;125(7):880–887.
28. Widdel L, Kleinschmidt-DeMasters BK, Kindt G. Tumor-to-tumor metastasis from hematopoietic neoplasms to meningiomas: report of two patients with significant cerebral edema. World Neurosurg 2010;74(1):165–171.
29. Mawrin C, Perry A. Pathological classification and molecular genetics of meningiomas. J Neurooncol 2010;99(3):379–391.
30. McKenzie CR, Rengachary SS, McGregor DH, Dixon AY, Suskind DL. Subdural hematoma associated with metastatic neoplasms. Neurosurgery 1990; 27(4):619–624; discussion 624–625.
31. Lui YW, Malhotra A, Farinhas JM, et al. Dynamic perfusion MRI characteristics of dural metastases and meningiomas: a pilot study characterizing the first-pass wash-in phase beyond relative cerebral blood volume. AJR Am J Roentgenol 2011;196(4): 886–890.
32. Lou X, Chen ZY, Wang FL, Ma L. MR findings of Rosai-Dorfman disease in sellar and suprasellar region. Eur J Radiol 2012;81(6):1231–1237.
33. Resnick DK, Johnson BL, Lovely TJ. Rosai-Dorfman disease presenting with multiple orbital and intracranial masses. Acta Neuropathol (Berl) 1996;91(5): 554–557.
34. Antuña Ramos A, Alvarez Vega MA, Alles JV, Antuña Garcia MJ, Meilán Martínez A. Multiple involvement of the central nervous system in Rosai-Dorfman disease. Pediatr Neurol 2012;46(1): 54–56.
35. Rosai J, Dorfman RF. Sinus histiocytosis with massive lymphadenopathy: a pseudolymphomatous benign disorder—analysis of 34 cases. Cancer 1972;30 (5):1174–1188.
36. Said R, Abi-Fadel F, Talwar J, Attallah JP, Dilawari A. Intracranial Rosai-Dorfman: a clinical challenge. Neurologist 2011;17(2):117–119.
37. Mahzoni P, Zavareh MHI, Bagheri M, Hani N, Moqtader B. Intracranial Rosai-Dorfman disease. J Res Med Sci 2012;17(3):304–307.
38. Mehraein Y, Wagner M, Remberger K, et al. Parvovirus B19 detected in Rosai-Dorfman disease in nodal and extranodal manifestations. J Clin Pathol 2006;59(12):1320–1326.
39. Rodriguez-Galindo C, Helton KJ, Sánchez ND, Rieman M, Jeng M, Wang W. Extranodal Rosai-Dorfman disease in children. J Pediatr Hematol Oncol 2004;26(1):19–24.
40. Raslan OA, Schellingerhout D, Fuller GN, Ketonen LM. Rosai-Dorfman disease in neuroradiology: imaging findings in a series of 10 patients. AJR Am J Roentgenol 2011;196(2):W187–W193.
41. Zhu H, Qiu LH, Dou YF, et al. Imaging characteristics of Rosai-Dorfman disease in the central nervous system. Eur J Radiol 2012;81(6):1265–1272.
42. Huang HY, Huang CC, Lui CC, Chen HJ, Chen WJ. Isolated intracranial Rosai-Dorfman disease: case report and literature review. Pathol Int 1998;48 (5):396–402.
43. Clarençon F, Bonneville F, Rousseau A, et al. Intracranial solitary fibrous tumor: imaging findings. Eur J Radiol 2011;80(2):387–394.
44. Carneiro SS, Scheithauer BW, Nascimento AG, Hirose T, Davis DH. Solitary fibrous tumor of the meninges: a lesion distinct from fibrous meningioma—a clinicopathologic and immunohistochemical study. Am J Clin Pathol 1996;106(2):217–224.
45. Johnson MD, Powell SZ, Boyer PJ, Weil RJ, Moots PL. Dural lesions mimicking meningiomas. Hum Pathol 2002;33(12):1211–1226.
46. Fargen KM, Opalach KJ, Wakefield D, Jacob RP, Yachnis AT, Lister JR. The central nervous system solitary fibrous tumor: a review of clinical, imaging and pathologic findings among all reported cases from 1996 to 2010. Clin Neurol Neurosurg 2011; 113(9):703–710.
47. Bisceglia M, Galliani C, Giannatempo G, et al. Solitary fibrous tumor of the central nervous system: a 15-year literature survey of 220 cases (August 1996–July 2011). Adv Anat Pathol 2011;18 (5):356–392.
48. Mekni A, Kourda J, Hammouda KB, et al. Solitary fibrous tumour of the central nervous system: pathological study of eight cases and review of the literature. Pathology 2009;41(7):649–654.
49. Rutten I, Raket D, Francotte N, Philippet P, Chao SL, Lemort M. Contribution of NMR spectroscopy to the differential diagnosis of a recurrent cranial mass 7 years after irradiation for a pediatric ependymoma. Childs Nerv Syst 2006;22(11): 1475–1478.
50. Sivendran S, Vidal CI, Barginear MF. Primary intracranial leiomyosarcoma in an HIV-infected patient. Int J Clin Oncol 2011;16(1):63–66.
51. Lerdlum S, Lalitanantpong S, Numkarunarunrote N, Chaowanapanja P, Suankratay C, Shuangshoti S. MR imaging of CNS leiomyosarcoma in AIDS patients. J Med Assoc Thai 2004;87(suppl 2): S152–S160.
52. Purgina B, Rao UN, Miettinen M, Pantanowitz L. AIDS-related EBV-associated smooth muscle tumors: a review of 64 published cases. Pathol Res Int 2011;2011:561548 .
53. Zevgaridis D, Tsonidis C, Kapranos N, Venizelos I, Tsitsopoulos P, Tsitsopoulos P. Epstein-Barr virus associated primary intracranial leiomyoma in organ transplant recipient: case report and review of the literature. Acta Neurochir (Wien) 2009;151(12): 1705–1709.
54. Bejjani GK, Stopak B, Schwartz A, Santi R. Primary dural leiomyosarcoma in a patient infected with human immunodeficiency virus: case report. Neurosurgery 1999;44(1):199–202.

55. Smith AB, Rushing EJ, Smirniotopoulos JG. Pigmented lesions of the central nervous system: radiologic-pathologic correlation. RadioGraphics 2009; 29(5):1503–1524.
56. Jellinger K, Böck F, Brenner H. Meningeal melanocytoma: report of a case and review of the literature. Acta Neurochir (Wien) 1988;94(1-2):78–87.
57. Rades D, Heidenreich F, Tatagiba M, Brandis A, Karstens JH. Therapeutic options for meningeal melanocytoma: case report. J Neurosurg 2001;95 (2,suppl):225–231.
58. Painter TJ, Chaljub G, Sethi R, Singh H, Gelman B. Intracranial and intraspinal meningeal melanocytosis. AJNR Am J Neuroradiol 2000;21(7): 1349–1353.
59. Takeuchi T, Sato M, Sonomura T, Itakura T. Erdheim-Chester disease associated with intramedullary spinal cord lesion. Br J Radiol 2012;85(1011): e62–e64.
60. Lachenal F, Cotton F, Desmurs-Clavel H, et al. Neurological manifestations and neuroradiological presentation of Erdheim-Chester disease: report of 6 cases and systematic review of the literature. J Neurol 2006;253(10):1267–1277.
61. Veyssier-Belot C, Cacoub P, Caparros-Lefebvre D, et al. Erdheim-Chester disease: clinical and radiologic characteristics of 59 cases. Medicine (Baltimore) 1996;75(3):157–169.
62. Sedrak P, Ketonen L, Hou P, et al. Erdheim-Chester disease of the central nervous system: new manifestations of a rare disease. AJNR Am J Neuroradiol 2011;32(11):2126–2131.
63. Drier A, Haroche J, Savatovsky J, et al. Cerebral, facial, and orbital involvement in Erdheim-Chester disease: CT and MR imaging findings. Radiology 2010;255(2):586–594.
64. Alfieri A, Gazzeri R, Galarza M, Neroni M. Surgical treatment of intracranial Erdheim-Chester disease. J Clin Neurosci 2010;17(12):1489–1492.
65. Martinez R. Erdheim-Chester disease: MR of intraaxial and extraaxial brain stem lesions. AJNR Am J Neuroradiol 1995;16(9):1787–1790.
66. Christoforidis GA, Spickler EM, Recio MV, Mehta BM. MR of CNS sarcoidosis: correlation of imaging features to clinical symptoms and response to treatment. AJNR Am J Neuroradiol 1999;20(4): 655–669.
67. Shah R, Roberson GH, Curé JK. Correlation of MR imaging findings and clinical manifestations in neurosarcoidosis. AJNR Am J Neuroradiol 2009;30(5): 953–961.
68. Rybicki BA, Major M, Popovich J Jr, Maliarik MJ, Iannuzzi MC. Racial differences in sarcoidosis incidence: a 5-year study in a health maintenance organization. Am J Epidemiol 1997;145(3):234–241.
69. Nowak DA, Widenka DC. Neurosarcoidosis: a review of its intracranial manifestation. J Neurol 2001; 248(5):363–372.
70. Smith JK, Matheus MG, Castillo M. Imaging manifestations of neurosarcoidosis. AJR Am J Roentgenol 2004;182(2):289–295.
71. Pawate S, Moses H, Sriram S. Presentations and outcomes of neurosarcoidosis: a study of 54 cases. QJM 2009;102(7):449–460.

RadioGraphics

From the Radiologic Pathology Archives
Mass Lesions of the Dura: Beyond Meningioma—Radiologic-Pathologic Correlation

Alice Boyd Smith, MD • Iren Horkanyne-Szakaly, MD • Jason W. Schroeder, LCDR, USN, MC • Elisabeth J. Rushing, MD

RadioGraphics 2014; 34:295–312 • **Published online** 10.1148/rg.342130075 • **Content Codes:** CT MR NR

Page 297
In contradistinction to meningioma, HPC can result in erosion of adjacent bone, as opposed to the hyperostosis that may accompany meningioma, and intratumoral calcification is not seen in HPC.

Page 300
Dural metastases are frequently solitary, potentially leading to a misdiagnosis of meningioma and delay in care.

Page 304
Leiomyoma and leiomyosarcoma should be included in the differential diagnosis of dural-based masses in AIDS patients.

Page 306–307
In a series by Drier et al, all of the patients with intracranial lesions had osteosclerosis of the sinus walls or orbital masses. Therefore, if lesions are also noted to involve the facial bones or orbits, it is suggestive of ECD.

Page 308–309
Owing to its nonspecific clinical presentation and neuroradiologic imaging characteristics, neurosarcoid is a difficult diagnosis to confirm, especially in the absence of systemic disease. Lumbar puncture may be useful in ruling out other neurologic disorders, but the findings in neurosarcoid are nonspecific (high protein, high leukocyte count, and normal or low glucose) and in up to 30% of cases may be normal. Performing chest imaging to evaluate for pulmonary involvement may be helpful.